Exploring the phycosphere of Emiliania huxleyi : from bloom dynamics to microbiome assembly experiments

Mariana Câmara dos Reis, Sarah Romac, Florence Le Gall, Dominique Marie, Miguel Frada, Gil Koplovitz, Thierry Cariou, Nicolas Henry, Colomban de Vargas, Christian Jeanthon

Exploring the phycosphere of *Emiliania huxleyi*: from bloom dynamics to microbiome assembly experiments

Mariana Câmara dos Reis[1,5+], Sarah Romac[1], Florence Le Gall[1], Dominique Marie[1], Miguel J. Frada[2,3], Gil Koplovitz[2], Thierry Cariou[4,*], Nicolas Henry[1,5,$], Colomban de Vargas[1,5], Christian Jeanthon[1,5+]

[1]Sorbonne Université/Centre National de la Recherche Scientifique, UMR7144, Adaptation et Diversité en Milieu Marin, Station Biologique de Roscoff, Roscoff, France

[2]The Interuniversity Institute for Marine Sciences in Eilat, 88103 Eilat, Israel

[3]Department of Ecology, Evolution and Behavior, Alexander Silberman Institute of Life Sciences, Hebrew University of Jerusalem, Israel

[4]Sorbonne Université/Centre National de la Recherche Scientifique, FR2424, Station Biologique de Roscoff, Roscoff, France

[5]Research Federation for the study of Global Ocean Systems Ecology and Evolution, FR2022/*Tara* GOSEE, Paris, France

*New address: IRD, US191, Instrumentation, Moyens Analytiques, Observatoires en Géophysique et Océanographie (IMAGO), Technopôle de Brest-Iroise, Plouzané, France

[$]New address: Sorbonne Université/Centre National de la Recherche Scientifique, FR2424, ABIMS bioinformatic platform, Station Biologique de Roscoff, Roscoff, France

+Corresponding authors: maricamarareis@gmail.com; jeanthon@sb-roscoff.fr

Running title: Microbiome assembly in *E. huxleyi* cultures

Abstract

Coccolithophores have global ecological and biogeochemical significance as the most important calcifying marine phytoplankton group. The structure and selection of prokaryotic communities associated with the most abundant coccolithophore and bloom-forming species, *Emiliania huxleyi*, are still poorly known. In this study, we assessed the diversity of bacterial communities associated with an *E. huxleyi* bloom in the Celtic Sea (Eastern North Atlantic), exposed axenic *E. huxleyi* cultures to prokaryotic communities derived from bloom and non-bloom conditions and followed the dynamics of their microbiome composition over one year. Bloom-associated prokaryotic communities were dominated by SAR11, Marine group II Euryarchaeota, Rhodobacterales and contained substantial proportions of known indicators of phytoplankton bloom demises such as Flavobacteriaceae and Pseudoalteromonadaceae. Taxonomic richness of bacteria derived from natural communities that associated with axenic *E. huxleyi* rapidly shifted and then stabilized over time. The succession of microorganisms recruited from the environment were consistently dependent on the composition of the initial bacterioplankton community. Phycosphere-associated communities derived from the *E. huxleyi* bloom were highly similar to one another, suggesting deterministic processes, whereas cultures from non-bloom conditions show an effect of stochasticity. Overall, this work sheds new light on the importance of the initial inoculum composition in microbiome recruitment and elucidates the temporal dynamics of its composition and long-term stability.

Key-words: Phytoplankton-bacteria interactions, microbiome assembly, phycosphere, metabarcoding, *Emiliania huxleyi*

Introduction

In the surface ocean, marine phytoplankton generate up to 50% of global primary production and at least half of this production is remineralized by marine heterotrophic bacteria (Falkowski, 1994; Field et al., 1998; Pomeroy et al., 2007). From an ecological perspective, interactions between these essential microbial groups are being increasingly recognized as a major force shaping microbial communities (Amin et al., 2015, Seymour et al., 2017). Phytoplankton-bacteria interactions are widespread in marine environments, in particular within the phycosphere, the region immediately surrounding individual phytoplankton cell (Bell & Mitchell, 1972; Smriga et al., 2016). This microscale region, analogous to the plant root rhizosphere, serves as the interface for phytoplankton-bacteria associations. Phytoplankton exudates fuel the activity of heterotrophic microorganisms, that in exchange can stimulate microalgal growth through the provision of growth hormones and vitamins (Amin et al., 2015, Croft et al., 2005), protection against pathogenic bacteria (Seyedsayamdost et al., 2014) and through the facilitation of iron uptake (Amin et al., 2009). In addition, phytoplankton release broad chemical classes of metabolites (Cirri & Pohnert, 2019) which can influence the taxonomy of phycosphere-associated bacteria (Buchan et al., 2014; Fu et al., 2020; Shibl et al., 2020).

Recent studies addressing the processes involved in bacterial community assembly in the phycosphere showed the influence of deterministic factors such as the place/time of isolation (Ajani et al., 2018) and the host species (Behringer et al., 2018; Lawson et al., 2018; Kimbrel et al., 2019; Sörenson et al., 2019; Jackrel et al., 2020; Mönnich et al., 2020). However, a combination between deterministic and stochastic effects in the microbiome recruitment process was also suggested (Kimbrel et al. 2019; Stock et al., 2022). To date, bacterial community composition and selection processes that influence the assembly of phycosphere

78 microbiomes are not well known in many phytoplankton, in part because of the micrometer
79 scale at which they take place (Kimbrel et al., 2019; Mönnich et al., 2020).
80 To overcome this challenge, possible strategies are to study the selection processes in
81 natural phytoplankton blooms (Zhou et al., 2019), in meso/microcosms or in cultures (Ajani et
82 al., 2018; Kimbrel et al., 2019; Sörenson et al., 2019; Fu et al., 2020; Mönnich et al., 2020),
83 when algal cells are at high concentrations. *Emiliania huxleyi* is the most abundant and
84 cosmopolitan coccolithophore species and is able to form massive annual blooms in temperate
85 and subpolar oceans mostly during Spring (Tyrrell & Merico, 2004). *E. huxleyi* blooms are
86 characterized by blue turquoise waters that can be observed from satellite images (Tyrrell &
87 Merico, 2004). These blooms have a critical importance for carbon and sulfur cycles due to the
88 ecological and biogeochemical roles of coccolithophores as primary producers, calcifiers, and
89 main contributors to the emission of dimethylsulfoniopropionate (DMSP) to the atmosphere
90 (Malin & Steinke, 2004; Rost et al., 2004). The potential role of viruses in bloom termination
91 has been thoroughly investigated (*e.g.* Bratbak, Egge & Heldal, 1993; Vardi et al., 2012;
92 Lehahn et al., 2014), but only few studies have targeted the microbial diversity associated with
93 *E. huxleyi* in natural environments (Gonzalez et al., 2000; Zubkov et al., 2001) and cultures
94 (Green et al., 2015; Orata et al., 2016; Rosana et al., 2016). The *Roseobacter*, SAR86 and
95 SAR11 lineages were identified as the main bacterial groups associated with natural *E. huxleyi*
96 blooms (Gonzalez et al., 2000; Zubkov et al., 2001). The co-occurrence of these groups could
97 be mediated by the presence of dimethylsulfoniopropionate (DMSP), produced and released
98 by *E. huxleyi* during blooms (Malin et al., 1993), which could be used as a sulfur compound
99 by bacteria (Miller & Belas, 2004; Tripp et al., 2008; Dupont et al., 2012). Meanwhile,
100 microbiomes of *E. huxleyi* in cultures are highly dominated by *Marinobacter* (Câmara dos Reis,
101 2021) and by Rhodobacteraceae (Green et al., 2015; Barak-Gavish et al., 2018).

In this study, we followed the dynamics of the prokaryotic community associated with *E. huxleyi* along a natural bloom in the Celtic Sea (Eastern North Atlantic) and used natural bloom and non-bloom samples from different depths to investigate the microbiome selection by an axenic *E. huxleyi* culture. We hypothesized that microbiomes recruited from bloom waters would be enriched in *Marinobacter* and Rhodobacteraceae, often associated with *E. huxleyi* cultures. Since composition can differ between surface and deep chlorophyll maximum (DCM) prokaryotic communities (Treusch et al., 2009; Allen et al., 2020; Mena et al., 2020) and is influenced by phytoplankton-bacteria interactions (Seymour et al., 2017), we also hypothesized that the recruited microbiomes would differ according to the initial prokaryotic composition.

Materials and Methods

Study site and sample collection

Samples used in this study were collected aboard the schooner *Tara* (Sunagawa et al., 2020) in the Celtic Sea (from 48°19-48°24 N/6°28-7°02 W; Fig. 1A and B), during the '*Tara* BreizhBloom' cruise from May 27 to June 2, 2019. To monitor the bacterial dynamics in an *E. huxleyi* bloom formed in this area, an Argo float (https://argo.ucsd.edu/) was deployed in the center of the bloom patch and its position was used twice a day (early morning and end of the afternoon) for 5 days to determine the geographical locations of the sampling stations.

On the last sampling day, an additional site about 34 km apart from the bloom area was also sampled (Fig. 1A). For each sampling event, surface to 50 m depth profiles of temperature, salinity, turbidity, pressure, photosynthetic active radiation (PAR), chlorophyll *a* (chla) fluorescence, oxygen concentrations and pH were conducted by deploying a SBE19+ profiler (Sea-Bird Scientific). Bloom depth, determined as the maximum turbidity depth, was generally very close to the DCM depth. Surface and bloom water samples were collected using an 8L

Niskin bottle for nutrient analyses. After collection, nutrient samples (125 mL) were stored at -20°C for further analysis. Concentrations of nitrate, nitrite, phosphate and silicate were measured using a AA3 auto-analyzer (Seal Analytical) following the methods described by Tréguer & Le Corre (1975) and Aminot & Kerouel (2007). Samples for flow cytometry (FCM), scanning electron microscopy (SEM), and metabarcoding analysis were collected at the bloom depth by pumping and prefiltered through a 20 µm mesh to eliminate large microplankton. For FCM analysis of photosynthetic eukaryotes and prokaryotic communities, two replicates (1.5 mL) were fixed using glutaraldehyde (0.25% final concentration) and Poloxamer 10% (0.1% final concentration) and incubated for 15 min at 4°C before flash freezing in liquid nitrogen. For SEM analysis, samples of morning sites (two replicates of 250 mL) were gently filtered onto polycarbonate membranes (47 mm in diameter; 1.2 µm pore-size) (Millipore). Filters were placed onto PetriSlides (Millipore), dried at least 2h at 50°C, and finally stored at room temperature. For metabarcoding analysis, cell biomass from bloom depth was collected from ~ 14 L of seawater by successive filtration onto large (142 mm in diameter) 3 µm pore-size and then 0.2 µm pore-size polycarbonate membranes (Millipore). Filters were flash-frozen in liquid nitrogen and stored at -80°C for later DNA analyses.

Scanning electron microscopy analysis

Representative filter portions were fixed in aluminum stubs and sputter coated with gold–palladium (20 nm) (Keuter et al., 2019). Quantitative assessment of *E. huxleyi* cells was performed using a Phenom Pro scanning electron microscope. Cells were counted in twenty random screens (area analyzed = 0.16 mm^2) and cell concentrations were calculated based on the filtered sample volume corresponding to the area analyzed (0.042 mL).

Community assembly experiments

(i) Axenization. The *E. huxleyi* strain RCC1212, obtained from the Roscoff Culture Collection, was axenized following a sequence of washing and centrifugation steps, and variable incubation periods with increasing concentrations of an antibiotic solution mixture (ASM) as detailed in the original protocol developed at the Scottish Association for Marine Science (Oban, UK) available at: https://www.ccap.ac.uk/wp-content/uploads/2020/06/KB_Antibiotic_treatment.pdf.

This method is briefly detailed in the Supplementary Materials and Methods section.

(ii) Sample preparation and inoculation. Four seawater samples were used in the bacterial community assembly experiment. They consisted of a surface and a DCM sample collected in the bloom area on day 5 (thereafter named inside bloom surface and inside bloom DCM) and a surface and a DCM sample collected the same day outside the bloom area (thereafter named outside bloom surface and outside bloom DCM) (Supplementary Fig. 1). In order to remove autotrophic picoeukaryotes and cyanobacteria from the inoculum, seawater samples were gently filtered through a 0.45 µm pore size membrane (Millex-HV, PVFD, Millipore). To estimate the number of prokaryotic cells lost during the filtration step, aliquots of total and filtered seawater samples were fixed for FCM analysis using the methods above. After filtration, 150 µL of each prokaryotic community (final cell concentration of about 6.8 x 10^3 cells/mL) were transferred in triplicates into 50 mL culture flasks filled with 15 mL of K/2 medium prepared as described in the Supplementary Materials and Methods. Finally, 150 µL of the axenic RCC1212 culture were added to each flask (final cell concentration of 3.8 x 10^3 cells/mL). Six flasks filled with 15 mL of K/2 medium and inoculated with 150 µL of the axenic RCC1212 culture were used as controls. In total, 18 cultures (3 replicates of 4 treatments and 6 controls) were incubated at 15°C and a 12:12 photoperiod regime. Due to space limitation, only one thermostatic chamber with a light intensity of 20 µmol photons $s^{-1}m^{-2}$ using a blue neutral density filter was available onboard for incubation.

(iii) Survey of the culture microbiomes. Back to the laboratory and 10 days after inoculation, which corresponds to the time needed by *E. huxleyi* cultures to reach the end of exponential growth phase, axenic status of controls was checked by FCM. Cultures (3 replicates of 4 treatments and one axenic control) were transferred by inoculating 100 µL of the culture in 10 mL of fresh K/2 medium every 11-14 days for the first 176 days of experiment and then every 3 weeks until its end (day 393). At each culture transfer and at the end of the experiment, treatments were sampled for FCM analyses and prokaryotic community composition analysis (3 replicates x 4 treatments x 8 DNA samplings = 96 samples) (Supplementary Fig. 1). The axenic control was regularly checked to ensure the clean handling of the cultures. In addition, culture flasks were randomized daily in the incubator to minimize positional effect on growth. For FCM, duplicate samples were fixed as previously described and analyses, performed according to Marie et al., (1999), are detailed in the Supplementary Materials and Methods section. For community composition analysis, 2 mL of culture was centrifuged at 2,000 *g* for 30 sec to reduce the microalgal load. Preliminary tests showed that this procedure reduces microalgal load while keeping most of the bacterial cells (about 90%). The supernatants were transferred into new tubes containing 2 µL of Poloxamer 188 solution 10% (Sigma-Aldrich) and centrifuged at 5,600 *g* for 5 min. The supernatants were discarded, and the pellets were stored at -80°C until DNA extraction.

DNA extraction, PCR amplification and sequencing

DNA extraction from environmental and culture samples and amplification steps used to amplify the prokaryotic 16S rRNA gene using the universal prokaryote primers 515F-Y (5'-GTGYCAGCMGCCGCGGTAA-3') labeled with eight-nucleotide tag unique to each sample at the 5' end and 926R (5'-CCGYCAATTYMTTTRAGTTT-3') (Parada et al., 2016) are detailed in the Supplementary Materials and Methods and in Romac (2022a, 2022b, 2022c,

2022d). The “tagged-PCR” approach was used (Bohmann et al., 2022). Briefly, DNA samples were PCR amplified using the above metabarcoding primers with 5′ nucleotide tags and following PCR amplification, the individually tagged PCR products were purified and pooled. Pools were sent to Fasteris SA (Plan-les-Ouates, Switzerland) where ligation-based library preparation was carried out and high-throughput sequencing was performed using Illumina Miseq paired-end sequencing technology (2x250). In total, three DNA pools were sequenced. The two first, containing the environmental samples and the first 84 experiment samples (first 7 time points) were sequenced in two independent Illumina runs (technical replicates). The last 12 experiment samples (day 393) were sequenced in another Illumina run without sequencing replicates.

Bioinformatics

The steps of library separation, removal of Illumina adapters and first quality control were performed by Fasteris SA (see Supplementary Materials and Methods). The detailed scripts used in this study can be downloaded from https://github.com/mcamarareis/microbiome_assembly. Briefly, raw reads from each sequencing run were demultiplexed based on the 8 nucleotide tag sequences with cutadapt (version 2.8.1) (Martin, 2011). The “tagged-PCR” approach we used generated half of both forward and reverse reads containing a P5 Illumina adapter and the other half a P7 adapter resulting in forward and reverse reads in both R1 and R2 files (mixed orientation). To deal with the presence of reads in mixed orientation in the R1 and R2 raw files, the demultiplexing was performed in two rounds (see details in Supplementary Materials and Methods). Then, primer sequences were removed using cutadapt (version 2.8.1) (Martin, 2011). Because sequences from different sequencing runs and from different sequencing cycles can have different error rates, they were processed independently to obtain an amplicon sequence variant (ASV) table

using the DADA2 pipeline (version 1.14.0 in R 3.6.1) (Callahan et al., 2016; R Core Team, 2017). The overall read quality of the demultiplexed primer-free sequences was first investigated with the DADA2 function *plotQualityProfile* to identify the position where the quality distribution dropped for R1 and R2 reads. Then, forward and reverse reads were trimmed where the quality decreased (i.e., at position 215 for R1 and at position 190 for R2 files) and reads with ambiguous nucleotides or with a maximum number of expected errors (maxEE) superior to 2 were filtered out using the function *filterAndTrim*. For each combination of runs and demultiplexing rounds, error rates were defined using the function *learnErrors* and denoised using the *dada* function in pooled mode before being merged with *mergePairs* (which generated ASVs of about 373 bp). Then, all the independent processed datasets were merged in one sequence table (for each sample, reads from the two rounds of demultiplexing were summed while reads coming from the two sequencing runs were kept separate) and processed for chimera removal using the function *removeBimeraDenovo*, also performed in pooled mode and with a "minFoldParentOverAbundance" of 8. The parameters used at each DADA2 step are specified in the Supplementary Table 1.

ASVs shorter than 366 bp and longer than 377 bp were filtered out, and the remaining ones were taxonomically assigned using IDTAXA (50% confidence threshold) with the Silva database v138 (Quast et al., 2013; Murali et al., 2018). Chloroplasts and mitochondrial ASVs were removed. ASVs not classified at the domain level by IDTAXA were assigned to the best hit in Silva v138 by pairwise global alignment (usearch_global VSEARCH's command) (Rognes et al., 2016). These ASVs were removed if they could not be classified and/or were classified as chloroplasts or mitochondrial sequences by VSEARCH (at 80% identity threshold). The resultant ASV table was filtered to remove ASVs accounting for less than 0.001% of the total number of reads (abundance filter). Consistency of technical replicates was evaluated by Procrustes analysis (function *procrustes* from vegan package), which measures

the similarity between two ordinations of the same objects, followed by a protest, which measures the significance of the correlation (Oksanen et al., 2015). For this, we used a comparative principal component analysis performed on the Hellinger transformed data. After consistency was confirmed ($p < 0.001$ and correlation = 0.99), independent technical replicates of each culture were merged by the sum of the number of reads of the ASVs present in the two replicates of the same culture (prevalence filter). The abundance and prevalence filters described above removed about 68% of the total number of ASVs while keeping 99% of the number of reads. The final dataset (filtered ASV table used for further analysis) contained 107 samples (11 from the environment and 96 from cultures) for a total of 6,017,019 reads and 294 prokaryotic ASVs.

Community composition and statistical analyses

(i) Environmental samples. All the analyses were conducted in R version 4.0.2 in Rstudio (1.1.442) and the plots were produced with ggplot2 (RStudio Team, 2016; Wickham, 2016; R Core Team, 2017). Taxonomy treemaps of environmental samples were produced at the genus level considering the best hits classified by VSEARCH. To facilitate visualization, low abundant genera (accounting to less than 3% of relative abundance at each sample) present at the raw community table were grouped. To compare environmental samples and cultures, mean alpha diversity indices (richness and Shannon index) were measured after rarefying the ASV table 100 times at the minimum number of reads (2,479) using the function *rtk* (Saary et al., 2017). Hierarchical cluster analysis (HCA) (method "ward.D2") was used to identify differences in the free-living prokaryotic communities by sites using the Hellinger distance (Euclidean distance of the Hellinger-transformed matrix; Legendre & Gallagher, 2001) using the function *hclust* from stats package (R Core Team, 2017).

(ii) Experiment. To analyze alpha diversity dynamics of the cultures, rarefaction was performed at a read depth of 5,957 reads using the same approach as for the environmental samples. For beta diversity analysis, the Jaccard dissimilarity was calculated on the rarefied table using the function *decostand* from vegan package. Hellinger distance was calculated from the non rarefied table also using the function *decostand* (Legendre & Gallagher, 2001). To explore beta diversity patterns, we performed a principal component analysis (PCA) on the Hellinger transformed data using the function *rda* from vegan. A principal coordinates analysis (PCoA) was performed using the Jaccard dissimilarity using the function *pcoa* from ape package (Paradis & Schliep, 2019). To test the influence of the treatments, replicates and time on the microbiome beta diversity, we performed a permutational analysis of variance (PERMANOVA) (Anderson, 2005). Before running the analysis, the functions *betadisper* from the package vegan and *anova*-like permutation test from stats package were used to identify significant deviations on the multivariate beta dispersion of the data for treatments, replicates, time and of the interaction between treatments and time (Oksanen et al., 2015). The effect of treatments and replicates (nested within treatments) was tested using the function *nested.npmanova* from the package BiodiversityR (Kindt & Coe, 2005). To test the effect of time and the interaction between treatments and time, we used the function *adonis* from vegan including treatments, replicates, and time (number of days) as fixed variables in the model, with permutations restricted to the replicates level. HCA was done using the Hellinger distance as previously described. Taxonomy barplots were produced by showing the three most abundant genera (considering the best hits classified by VSEARCH), while the less abundant were merged as "others". *IndVal* analyses were run with the rarefied table to identify indicative species of the three groups of treatments evidenced in the beta diversity analysis (inside and outside bloom DCM and both surface samples) using the function *multipatt* from the package indicspecies v1.7.9 with 10,000 permutations (De Cáceres and Legendre, 2009). P-values were

adjusted for multiple comparisons using the false discovery rate method using the function *p.adjust* from the package stats.

Results

Physico-chemical parameters and bacterial community structure dynamics in the *E. huxleyi* bloom

Coccolithophore blooms occur seasonally from April to June in the Bay of Biscay along the continental shelf to the Celtic Sea (Holligan et al., 1983; Poulton et al., 2014; Perrot et al., 2018). Here, we followed and sampled an *E. huxleyi* bloom for a week from end of May to early June 2019 in the Celtic Sea (Fig. 1A and 1B) using near-real time interpolated images of non-algal suspended particulate matter (SPM) derived from MERIS and MODIS satellite reflectance data (Perrot et al., 2018; Gohin et al., 2019) as provided by Ifremer (http://marc.ifremer.fr/en) .

During the 5-day sampling period, temperature and salinity ranged from 12.4°C to 15.4°C and from 35.4 to 35.5 PSU, respectively (Supplementary Table 2). In both inside and outside bloom waters, nutrient concentrations were low with NO_2 + NO_3 and PO_4 ranging from the detection thresholds to 1.25 µmol and 0.05 to 0.2 µmol/L, respectively. These low values were typical of a bloom event where cells consume most of the nutrients. *E. huxleyi* whose cell densities ranged from 1.6 x 10^3 to 5.6 x 10^3 cells/mL within bloom waters (Fig. 1C) dominated the total photosynthetic eukaryotic community (2.5 x 10^4 cells/mL on average). In these samples, total numbers of heterotrophic bacteria varied from 8.1 x 10^5 to 2.0 x 10^6 cells/mL (Fig. 1D) whereas the lowest prokaryotic cell concentration was measured in the outside bloom sample (Fig. 1D and Supplementary Table 2).

Overall, the inside and outside bloom DCM samples displayed a prokaryotic richness of about 140 ± 29ASVs (mean ± SD, n=11) (Fig. 2A). Richness increased over the course of

the bloom, reaching a maximum at day 4. The DCM samples collected on day 5 inside and outside the bloom for the community assembly experiments contained 148 and 133 ASVs, respectively. The Shannon diversity index displayed homogeneous values (mean 4.1 ± 0.2) across samples (Fig. 2B).

Hierarchical clustering revealed 3 groups of sampling periods, the first one comprising samples from day 1 to day 2 AM, the second grouping those of day 2 PM and day 3 AM, and the third clustering those of day 3 PM to day 5 PM. These successive sampling periods reflected the distinct shifts in the bacterial community during the bloom and may be related to the bloom development (Supplementary Fig. 2). During the whole bloom survey, mean abundances of prokaryotic communities inside the bloom showed that Proteobacteria (64% of the total of reads) and Bacteroidota (15%) were the two major dominant phyla, followed by Cyanobacteria (7%), Thermoplasmatota (4%), and Verrucomicrobiota (4%). Pelagibacteraceae (15%), Pseudoalteromonadaceae (12%) and Rhodobacteraceae (12%) were the most abundant proteobacterial families while Flavobacteriaceae (11%) dominated within the Bacteroidota. Among the dominant genera, abundances of SAR11 clade Ia (about 10% of the total reads), Synechococcus sp. (7%), SAR86 clade (5%), and uncultured Rhodobacteraceae members (4%) remained stable along the bloom survey (Supplementary Fig. 3). Several other genera demonstrated substantial abundance shifts. *Ascidiaceihabitans* and *Sulfitobacter*, accounting for 7% in the first sampling period, decreased in the second and third sampling periods. *Nitrosopumilus* (Thaumarchaeota), Thermoplasmata (Marine group II euryarchaeota), *Vibrio* and *Pseudoalteromonas* exhibited an inverse pattern. As low as 2% or less in the first sampling period, their abundance increased significantly (9 to 14%) in the second sampling period. *Pseudoalteromonas* proportions persisted (14%) in the third sampling period while those of other taxa decreased to their initial numbers. Not detected or at very low abundance in the first sampling periods, *Alteromonas* peaked (up to 4%) only at the end of the bloom survey.

On day 5, prokaryotic communities outside the bloom grouped with those collected inside the bloom area (Supplementary Fig. 2). In both samples, the fourth most abundant taxa making up to >44% of the total reads were identical and displayed very close proportions (*Pseudoalteromonas* 19% and 21% in inside and outside bloom, respectively, *Synechococcus* 9% and 7%, SAR11 clade Ia 8% and 11%, and *Alteromonas* 8% in both samples). The main compositional differences these samples that served as inocula for the community assembly experiment were the abundance of *Lentimonas* (5% inside vs 2% outside bloom), and of the OM60 (NOR5) clade and Marine group II members (each of them accounting for 2% inside vs 4% outside bloom). Relative abundances of the clades that were recruited from these samples during the experiment were lower and close in both samples (OM43 clade, 1.5% and 2.3% in inside and outside bloom, respectively; KI89A clade, 0.6% and 0.4%; *Luminiphilus*, 0.7% and 0.3%; *Aurantivirga*, 0.1% and 0.3%; *Polaribacter*, 0.5% and 0.2%) or similar (SAR92 clade, 1.5%).

Community assembly experiment

(i) Dynamics of cell concentrations and alpha diversity patterns

Seawater samples used to inoculate axenic *E. huxleyi* cultures were filtered through 0.45 µm membranes to remove phototrophs (autotrophic eukaryotes and *Synechococcus* populations) and overcome their effects on microbiome assembly. FCM analysis demonstrated that about 40% of the initial bacterial cell concentration was lost after this filtration step. As addressed in the Discussion, we acknowledge that this step may have also biased the bacterial composition in the inocula. Due to limited incubation space onboard, cultures were incubated at low light (20 µmol photons $s^{-1}m^{-2}$) and these light conditions were maintained during the first weeks of incubation. However, a drastic decrease (~ 80%) of *E. huxleyi* cell concentrations was observed in all the treatments between the day 10 and day 33 (Supplementary Fig. 4A).

To avoid culture crash, we increased the light intensity to 70 ± 20 µmol photons $s^{-1}m^{-2}$ and larger microalgal inocula (10% of the final culture volume instead of 1%) were used to transfer the cultures at day 33. *E. huxleyi* cell densities gradually increased at each subsequent transfer until day 71. At that point, they reached the highest cell concentration ($9.9 \times 10^5 \pm 1.2 \times 10^5$ cells/mL) and remained stable up to the end of the experiment (Supplementary Fig. 4A). Bacterial cell concentrations followed an opposite trend during the first weeks of incubation. After a rapid increase (~94%) from day 10 to 47, they decreased once *E. huxleyi* abundance became higher and remained relatively stable up to the end of the experiment (Supplementary Fig. 4B).

Regarding the structure of the bacterial community, a severe loss of richness was observed between the environmental and culture samples (Fig. 2A). At day 10, the bacterial richness in the cultures was about one fifth of the richness in the natural samples (30 ± 8 SD, n=12) (Fig. 2A). This reflected a parallel decrease in the Shannon index, which at day 10, was about one third the values recorded in environmental samples (1.4 ± 0.6 SD, n=12, Fig. 2B). Over the course of the experiment, we observed a decrease in richness along the first five weeks (mean decrease 25 ± 7 SD, n=12, until day 47) (Fig. 2A and Supplementary Fig. 4C). After an increase at day 59 that corresponded to the period of culture recovery, the richness values decreased again and remained stable until day 393 (12 ASVs ± 2). The decrease of richness was mainly associated with the loss of low abundance ASVs, while the dominant ones remained over the course of the experiment (Supplementary Fig. 5). In general, the Shannon index also decreased over the from day 10 to day 33 (mean decrease of 0.5 ± 0.6 SD, n=12) and then gradually increased to values (i.e. 1.2 ± 0.4 at day 393, n=12) similar to that from day 22. The highest richness and Shannon indexes were obtained in the treatments amended with the inside bloom DCM sample (richness, 26 ± 12 ASVs; Shannon, 1.6 ± 0.4, n=24).

Dynamics of beta diversity patterns in recruited microbiomes

In order to identify the influence of the different initial prokaryotic community composition and to follow the changes in the microbiome beta diversity with time, we used two metrics, the Hellinger distance (Euclidean distance of Hellinger-transformed data) and the Jaccard dissimilarity. PCoA using Jaccard dissimilarity demonstrated that *E. huxleyi* cultures inoculated with surface samples grouped together (Fig. 3A), while those inoculated with inside and outside bloom DCM samples formed two other independent clusters.

Statistical significance of the effect of treatments, replicates and time, as well as the interaction of treatment and time on the diversity of the microbiomes was assessed by PERMANOVA and nested PERMANOVA. Before performing PERMANOVA analysis we tested the beta-dispersion (variance) of the microbiomes grouped by treatments, time, treatments over time, and replicates. The dispersions (variance) of treatments as well as the interaction of treatments over time were not homogeneous for both metrics tested ($p < 0.05$). On the other hand, dispersions were likely homogeneous over time and across replicates ($p > 0.05$). Still, PERMANOVA results were robust to dispersion for balanced designs like ours (Anderson & Walsh, 2013). PERMANOVA results of Hellinger and Jaccard dissimilarities showed that significant proportions of the variance in microbiome composition among samples were explained by treatments (31% and 25%, respectively), replicates (31% and 15%, respectively), and time (6% and 7%, respectively) ($p < 0.01$) (Fig. 3B, Supplementary Tables 3 and 4). Although the interaction between treatments and time was significant using Hellinger distance ($F = 2.23$; $p = 0.016$), it explained a small proportion of the variance (2.5%).

Clustering using Hellinger distance revealed that the prokaryotic community composition of all the cultures grouped into three major clusters (Fig. 3C) supporting the PCoA using Jaccard dissimilarity results. Based on the Hellinger distance, the outside bloom DCM treatment samples (cluster a) formed two subclusters, highlighting the compositional

differences between the 3 replicates. Replicate 1 was dominated by *Alcanivorax* (78%, n=8), while *Erythrobacter* prevailed in replicate 2 (88%) and 3 (45%). Cluster b mainly consisted of microbiomes recruited from both surface water samples. Surface treatments were dominated by bacteria related to OM43, KI89A, and SAR92 clades, and to *Luminiphilus*. The third main cluster (c) entirely formed by microbiomes from the inside bloom DCM treatment was dominated by members of the OM43 (29%), KI89A (28%), SAR92 clade and *Polaribacter* (11% each). With the exception of those related to *Sulfitobacter*, *Luminiphilus,* OM43 and the OM60(NOR5) clades, ASVs that dominate (≥ 1%) in the cultures amended with inside and outside bloom DCM samples were generally low in abundance or not detected in the initial bacterioplankton community (Supplementary Fig. 6).

The number of indicative ASVs for each treatment varied widely and was significantly higher (21 out of 29) in cultures amended with inside bloom DCM waters (Supplementary Table 5). Flavobacteriales, with *Aurantivirga* and *Polaribacter* in particular, was the order containing the most indicative ASVs of microbiomes recruited from the inside bloom DCM sample. Members of SAR92 and KI89 clades displayed high *Indval* indexes in both inside bloom DCM and surface samples. The indicator ASVs of outside bloom DCM treatment were related to *Erythrobacter*, *Alcanivorax*, and OM60(NOR5) clade.

Besides the compositional differences among treatments, we observed a somewhat cyclic pattern of the beta-diversity over time using Hellinger distance (Fig. 4). Microbiome community compositions clearly differed from each other from days 10, 22 and 33 for all treatments, but they gradually tended to become similar to their initial status at the following time-points. This cyclic pattern was observed for inside and outside bloom surface treatments (Fig. 4A and C) and was particularly evident in the inside bloom DCM treatment (Fig. 4B). In these treatments, the dynamic was mainly driven by the dominance of the OM43 clade (ASV1) during the alga crash. In the algal growth recovery phase, the increased abundance of

Luminiphilus (ASV6) in surface treatments and of *Aurantivirga* (ASV12) and *Polaribacter* (ASV15) in inside bloom DCM cultures were also involved (Supplementary Fig. 7). The contributions of these ASVs were also supported by the PCAs species loadings. No cyclic pattern was observed for outside bloom DCM cultures (Fig. 4D). Instead, in line with hierarchical clustering results (Fig. 3C), dissimilarities in these cultures were higher between replicates than over time.

Discussion

In this study, we monitored the diversity of bacterial communities associated with an *E. huxleyi* bloom in the Celtic Sea, and collected bacterioplankton samples for conducting a microbiome selection experiment in axenic *E. huxleyi* cultures.

Prokaryotic communities associated to the demise phase of the *E. huxleyi* bloom

The composition of the bacterial community, *i.e.* the presence of Flavobacteriaceae, Pseudoalteromonadaceae, Alteromonadaceae and members of the genus *Sulfitobacter*, indicated that the *E. huxleyi* bloom had already entered the decaying phase when we started the sampling (Lovejoy et al., 1998; Buchan et al., 2014). Indeed, Flavobacteriia are reported amongst the main bacteria present in the declining phase of phytoplankton blooms (Teeling et al., 2012, 2016; Landa et al., 2016), which seems linked to their capacity to degrade high molecular weight substrates such as proteins and polysaccharides (Cottrell and Kirchman, 2000; Kirchman, 2002; Fernández-Gomez et al., 2013; Kappelmann et al., 2019; Francis et al., 2021). Furthermore, the algicidal effects of *Pseudoalteromonas*, *Alteromonas*, and *Sulfitobacter* strains and species have been documented in many microalgae including *E. huxleyi* (Holmström & Kjelleberg, 1999; Meyer et al., 2017; Li et al., 2018; Barak-Gavish et al., 2018), which calls attention to their potential role in the *E. huxleyi* bloom termination

(Lovejoy et al., 1998; Barak-Gavish et al., 2018). Satellite images and post-cruise analyses support that we started sampling the bloom in its decline phase. First, the high reflectance patch visible on the satellite images (Fig. 1A) and the daily vanishing of the coccolith-derived turbidity signal observed from the interpolated images of non-algal SPM were both indicative of detached coccoliths from dead *E. huxleyi* cells (Neukermans & Fournier, 2018; Perrot et al., 2018). This assumption was confirmed by the complete disappearance of the coccolith-derived turbidity signal a couple of days after we left the sampling area. Second, a suite of ongoing experiments on the bloom samples using diagnostic lipid- and gene-based molecular biomarkers (Vardi et al., 2009; Hunter et al., 2015; Ziv et al., 2016; Vincent et al., 2021) revealed the detection of specific viral polar lipids and visualized *E. huxleyi* infected cells during bloom succession, suggesting that Coccolithovirus infections may have partially participated in the demise of *E. huxleyi* bloom (F. Vincent, C. Kuhlisch, G. Schleyer, pers. comm.) as often proposed (Bratbak et al., 1993; Vardi et al., 2012; Laber et al., 2018).

As the bloom decline progressed, rapid and important shifts of the prokaryotic community were observed, probably reflecting a direct response by certain bacterial taxa to specific *E. huxleyi*-derived organic matter. Senescence compounds from decaying *E. huxleyi* cells probably fueled members of the genus *Ascidiaceihabitans* (formerly Roseobacter OCT lineage) (Wemheuer et al., 2015), whose relative abundances typically fluctuate during phytoplankton blooms (Hahnke et al., 2015; Lucas et al., 2016; Chafee et al., 2018; Choi et al., 2018) and promoted other functionally different transient taxa that represent key prokaryotic members during bloom decline. Among them, Thermoplasmata are generally associated with protein and lipid degradation (Orellana et al., 2019) while *Nitrosopumilus* may be favored by nitrite accumulation caused by algal release (Kim et al., 2019). The opportunistic *Vibrio* was among the most rapidly responding bacterial heterotrophs in the bloom termination conditions, likely degrading organic matter released from algal cells (Eiler *et al*., 2007) while *Alteromonas*

sp. have the metabolic capacity to degrade a diverse set of complex compounds like polysaccharides during the later stages of the bloom (Reintjes et al., 2019).

Community composition of environmentally recruited *E. huxleyi* microbiomes

Since our primary objective was to study the bacterial community selection and assembly by a single phytoplankton host, we used a filtration step to discard autotrophic phytoplankton cells, such as *Synechococcus* and picoeukaryotes abundantly represented in the initial planktonic communities (Supplementary Table 2). We acknowledge that this filtration strategy has removed large and particle-attached prokaryotes, the latter probably being abundant in the demise phase of the bloom, and has induced substantial modifications in the initial community composition of the inocula and finally in recruited microbiomes. Indeed, some of the main taxonomic groups recruited in the treatments were not previously reported in *E. huxleyi* and other phytoplankton cultures or in low abundance, notably *Luminiphilus*, and the clades SAR92, KI89A and OM43 (Green et al., 2015; Câmara dos Reis, 2021). Except members of the OM43 clade (Yang et al., 2016), these bacteria are known as important groups of oligotrophic marine Proteobacteria that do not usually grow in the rich organic matter conditions provided in phytoplankton-derived cultures (Cho & Giovannoni, 2004; Spring & Riedel, 2013). Another unexpected result of our study is the very low representation of *Marinobacter* sp. in the recruited microbiomes whereas previous studies have reported their dominance in cultures of worldwide *E. huxleyi* isolates (Green et al., 2015; Câmara dos Reis, 2021). We found them in low abundance in inside and outside bloom waters (0.15-0.2%), similar to multiyear average values (0.18%) in the Western English Channel (Gilbert et al., 2012). Since *Marinobacter* can be closely associated with particulate organic matter, including the eukaryotic phytoplankton population (Sonnenschein et al., 2012; Thompson et al., 2020), we cannot fully exclude the possibility that the filtration step impacted the abundance of

526 *Marinobacter* in the inocula and finally in the *E. huxleyi* cultures. A more likely hypothesis
527 however is that low light conditions might have induced algal cell death promoting the release
528 of methylated compounds (Reese et al., 2019; Fisher et al., 2020). The release of methylated
529 compounds by *E. huxleyi* may have provided a selective advantage to the specialist OM43
530 clade methylotrophs (Neufeld et al., 2008), dominant in all the cultures, and to other less
531 common bacterial taxa in the absence of strong competitors such as *Marinobacter*. This
532 hypothesis is in line with the opposite dynamics of *E. huxleyi* (decrease) and bacteria (increase)
533 coupled to the sharp decrease of the bacterial alpha diversity during the first month of culture,
534 indicating that a few bacterial taxa were outcompeting others. Despite the above limitations,
535 the high reproducibility of microbiome community composition across the biological replicates
536 suggests that they did not alter the general conclusions raised from our study.

537 Our results illustrate the importance of niche differentiation in natural communities.
538 Indeed, although no major differences were observed between environmental inside and
539 outside bloom bacterial communities, *E. huxleyi* microbiomes recruited from these samples
540 differed. Similarly, although we did not analyze the initial bacterial composition of epipelagic
541 surface samples (collected 34 km apart), they converged towards similar compositions,
542 dominated by *Luminiphilus*, SAR92, KI89A and OM43 clades. Other microbiome studies of
543 phytoplankton cultures have highlighted the impact of the initial community composition on
544 microbiomes after short (Ajani et al., 2018; Sörenson et al., 2019; Jackrel et al., 2020), and
545 long-term selection (Behringer et al., 2018). Remarkable features were found in the
546 microbiomes resulting from inside bloom DCM waters where several indicative flavobacterial
547 ASVs, mainly assigned to *Polaribacter* and *Aurantivirga*, were initially selected and remained
548 among the most prevalent and abundant ASVs after growth recovery of the host. Both genera
549 were identified as the main degraders of polysaccharides during diatom blooms (Krüger et al.,
550 2019) and showed clear successions along the bloom stages (Teeling et al., 2012; Landa et al.,

2016; Krüger et al., 2019; Liu et al., 2020). This may be related to the differential capacity of these bacteria to degrade phytoplankton-derived polysaccharides during blooms (Teeling et al., 2012; Krüger et al., 2019; Avci et al., 2020; Francis et al., 2021). Interestingly, SAR92 and *Luminiphilus* were also identified as important degraders of algal polysaccharides in bloom conditions (Francis et al., 2021), suggesting their potential functional role in our cultures.

We observed contrasting results between the inside and outside bloom DCM recruited microbiomes that can be linked to the origin of the samples. First, recruited microbiomes from inside bloom DCM samples were more diverse and displayed higher number of indicative ASVs, probably reflecting the higher diversity observed in the original seawater (Fig.2). We assume that exopolysaccharides/exudates of axenic *E. huxleyi* cultures have strongly influenced the recruited microbiomes and their long-term stability. We hypothesize that the higher diversity conferred stability to the microbiomes allowing the recovery after disturbance. This may likely explain the almost complete cyclic pattern they followed (Fig. 4B). Such cyclic patterns were shown in the surface microbiome of the seaweed *Delisea pulchra* (Longford *et al*., 2019) after experimental disturbances. These authors hypothesized that the production of halogenated furanones by the red algae exert a selective force for the establishment and persistency of early-colonizing bacteria which may protect the host against the colonization of pathogenic bacteria in later successional stages (Longford et al., 2019). In line with our data, this study favored the view that higher diversity in disturbed microbiomes may be a source of stability and resilience against perturbation (Longford et al., 2019). We consistently observed cyclic patterns in treatments having a high degree of uniformity in the replicates. This was not the case for the outside bloom DCM cultures whose bacterial communities displayed high levels of between-replicate variability.

Our study suggests the combined effect of deterministic processes and stochasticity on the microbiome assembly. The significant imprint of the original community in the inside

bloom DCM treatments suggests that deterministic processes (*e.g.* pre-exposition to algal exudates in the bloom assemblages adapted to *E. huxleyi* bloom exudates) influenced the final microbiome composition. On the other hand, variable communities grown from outside bloom DCM treatment are consistent with stochastic assembly overwhelming any signal of ecological selection. In line with our results, both deterministic and stochastic processes were found to influence community assembly in both the surface and DCM waters of the South Pacific Gyre (Allen et al., 2020). Homogeneous selection was the dominant community assembly process at both depths. However, stochastic processes had more effect at the DCM than in the temporally stable surface waters, presumably due to the greater influence of vertical nutrient supply and higher productivity and lower influence of horizontal dispersal (Allen et al., 2020 and references therein).

Conclusions

In this work, we combined an observational and an experimental approach to reveal the bacterial community structure in an *E. huxleyi* bloom and to address whether different microbial composition could influence microbiome assembly in a *E. huxleyi* culture. Our environmental data showed that the *E. huxleyi* bloom created unique ecological conditions favoring the combination of bacterial and archaeal groups that followed a clear successional trajectory. This trajectory suggests both potential algicidal bacteria-algae interactions and niche specialization by different taxa possibly corresponding to different stages in the successive degradation of *E. huxleyi*-derived organic compounds. Our experimental approach showed that the compositional homogeneity of the prokaryotic community of an *E. huxleyi* bloom in the demise phase influenced community assembly through deterministic processes. We showed that the source of the initial bacterioplankton communities influences the resulting composition of *E. huxleyi* microbiomes. Further studies using diverse phytoplankton cultures isolated from

a variety of oceanic regions and different trophic regimes could be useful to disentangle deterministic and stochastic factors driving microbiome assembly in the marine environment. Axenic phytoplankton cultures also represent a valuable resource to explore phytoplankton-bacteria interactions. Co-cultivation of isolates corresponding to indicative ASVs and *E. huxleyi* will be helpful to decipher how they interact. Future analyses combining transcriptomic and metabolomic analyses will provide valuable information about the genes and molecules involved in these ecologically key interactions.

Acknowledgments

This work was supported by a PhD fellowship from Sorbonne University and the Région Bretagne to MCdR, the Centre National de la Recherche Scientifique (CNRS, France), and the French Government ‘‘Investissements d’Avenir’’ programmes OCEANOMICS (ANR-11-BTBR-0008). We are grateful to the *Tara* Ocean Foundation, led by Romain Troublé and Etienne Bourgois, for the sampling opportunity and facilities onboard *Tara*, and to all the scientific and logistic team involved in the *Tara* Breizh Bloom cruise, notably captain Martin Herteau and his crew. We warmly thank Shai Fainsod, Michel Flores, Eric Pelletier, Daniella Schatz and Flora Vincent, for their contribution during the cruise, and Lydia White for her help in the statistical analysis. We are thankful to the Roscoff Bioinformatics platform ABiMS (http://abims.sb-roscoff.fr), part of the Institut Français de Bioinformatique (ANR-11-INBS-0013) and BioGenouest network, for sharing computing and storage resources, Eric Macé and INSU (Parc National d’Instrumentation Scientifique) for supplying the SBE19+ profiler, and to the RCC for providing the *E. huxleyi* cultures.

Data Accessibility

Genetic data and sample metadata:

Environmental samples are deposited in the bioproject PRJEB50692. Reads are deposited under the accession numbers ERX9644183 - ERX9644242 and biosamples under the accession numbers ERS10466567-ERS10466596.

Samples from the assembly experiment are deposited in the bioproject PRJEB48747. Reads are deposited under the accession numbers ERX9767825 - ERX9768004 and biosamples under the accession numbers ERS10539058-ERS10539153.

Author Contributions

CJ, MCdR, CdV designed the research. MCdR, CJ and SR participated on the sampling cruise. MCdR and CJ collected the DNA and transferred the cultures. FLG, SR, CJ produced the genetic data. MJF and GK analyzed the SEM filters. DM and MCdR analyzed the FCM samples. TC analyzed the nutrients samples. MCdR and NH analyzed the results. MCdR, CJ and CdV wrote the paper. All authors contributed to the discussions that led to the final manuscript, revised it and approved the final version.

References

Ajani, P. A., Kahlke, T., Siboni, N., Carney, R., Murray, S. A. & Seymour, J. R. (2018). The Microbiome of the Cosmopolitan Diatom Leptocylindrus Reveals Significant Spatial and Temporal Variability. In *Frontiers in Microbiology* (Vol. 9, p. 2758). https://www.frontiersin.org/article/10.3389/fmicb.2018.02758

Allen, R., Hoffmann, L. J., Larcombe, M. J., Louisson, Z. & Summerfield, T. C. (2020). Homogeneous environmental selection dominates microbial community assembly in the oligotrophic South Pacific Gyre. *Molecular Ecology*, *29*(23), 4680–4691.

Amin, S. A., Green, D. H., Hart, M. C., Kupper, F. C., Sunda, W. G. & Carrano, C. J. (2009). Photolysis of iron-siderophore chelates promotes bacterial-algal mutualism. *Proceedings of the National Academy of Sciences*, *106*(40), 17071–17076. https://doi.org/10.1073/pnas.0905512106

Amin, S. A., Hmelo, L. R., Van Tol, H. M., Durham, B. P., Carlson, L. T., Heal, K. R., Morales, R. L., Berthiaume, C. T., Parker, M. S., Djunaedi, B., Ingalls, A. E., Parsek, M. R., Moran, M. A. & Armbrust, E. V. (2015). Interaction and signalling between a cosmopolitan phytoplankton and associated bacteria. *Nature*, *522*(7554), 98–101. https://doi.org/10.1038/nature14488

Aminot, A. & Kérouel, R. (2007). *Dosage automatique des nutriments dans les eaux marines: méthodes en flux continu*. Editions Quae.

Anderson, M J. (2005). *PERMANOVA. Permutational multivariate analysis of variance. Department of Statistics, University of Auckland, Auckland*.

Anderson, Marti J. & Walsh, D. C. I. (2013). PERMANOVA, ANOSIM, and the Mantel test in the face of heterogeneous dispersions: What null hypothesis are you testing? *Ecological Monographs*, *83*(4), 557–574. https://doi.org/10.1890/12-2010.1

Avcı, B., Krüger, K., Fuchs, B. M., Teeling, H. & Amann, R. I. (2020). Polysaccharide niche partitioning of distinct Polaribacter clades during North Sea spring algal blooms. *The ISME Journal*, *14*(6), 1369–1383. https://doi.org/10.1038/s41396-020-0601-y

Barak-Gavish, N., Frada, M. J., Ku, C., Lee, P. A., DiTullio, G. R., Malitsky, S., Aharoni, A., Green, S. J., Rotkopf, R., Kartvelishvily, E., Sheyn, U., Schatz, D. & Vardi, A. (2018). Bacterial virulence against an oceanic bloom-forming phytoplankter is mediated by algal DMSP. *Science Advances*, *4*(10), eaau5716. https://doi.org/10.1126/sciadv.aau5716

Behringer, G., Ochsenkühn, M. A., Fei, C., Fanning, J., Koester, J. A. & Amin, S. A. (2018). Bacterial communities of diatoms display strong conservation across strains and time. *Frontiers in Microbiology*, *9*(APR). https://doi.org/10.3389/fmicb.2018.00659

Bell, W. & Mitchell, R. (1972). Chemotactic and growth responses of marine bacteria to algal extracellular products. *The Biological Bulletin*, *143*(2), 265–277. https://doi.org/10.2307/1540052

Bratbak, G., Egge, J. K. & Heldal, M. (1993). Viral mortality of the marine alga Emiliania huxleyi (Haptophyceae) and termination of algal blooms. *Marine Ecology Progress Series*, *93*(1–2), 39–48. https://doi.org/10.3354/meps093039

Bohmann, K., Elbrecht, V., Carøe, C., Bista, I., Leese, F., Bunce, M., Yu, D. W., Seymour, M., Dumbrell, A. J. & Creer, S. (2022). Strategies for sample labelling and library preparation in DNA metabarcoding studies. *Molecular Ecology Resources*, *22*(4), 1231–1246. https://doi.org/https://doi.org/10.1111/1755-0998.13512

Buchan, A., LeCleir, G. R., Gulvik, C. A. & González, J. M. (2014). Master recyclers: features and functions of bacteria associated with phytoplankton blooms. In *Nature reviews. Microbiology* (Vol. 12, Issue 10, pp. 686–698). https://doi.org/10.1038/nrmicro3326

Callahan, B. J., McMurdie, P. J., Rosen, M. J., Han, A. W., Johnson, A. J. A. & Holmes, S. P.

(2016). DADA2: High-resolution sample inference from Illumina amplicon data. *Nature Methods*, *13*, 581. https://doi.org/10.1038/nmeth.3869

Câmara dos Reis, M. (2021). *Structure and assembly of bacterial microbiomes in the Emiliania huxleyi phycosphere* [Sorbonne Université]. http://www.theses.fr/2021SORUS077/document

Chafee, M., Fernàndez-Guerra, A., Buttigieg, P. L., Gerdts, G., Eren, A. M., Teeling, H. & Amann, R. I. (2018). Recurrent patterns of microdiversity in a temperate coastal marine environment. *ISME Journal*, *12*(1), 237–252. https://doi.org/10.1038/ismej.2017.165

Cho, J.-C. & Giovannoni, S. J. (2004). Cultivation and growth characteristics of a diverse group of oligotrophic marine Gammaproteobacteria. *Applied and Environmental Microbiology*, *70*(1), 432–440.

Choi, D. H., An, S. M., Yang, E. C., Lee, H., Shim, J., Jeong, J. & Noh, J. H. (2018). Daily variation in the prokaryotic community during a spring bloom in shelf waters of the East China Sea. *FEMS Microbiology Ecology*, *94*(9), fiy134.

Cirri, E. & Pohnert, G. (2019). Algae−bacteria interactions that balance the planktonic microbiome. *New Phytologist*, *223*(1), 100–106. https://doi.org/10.1111/nph.15765

Cottrell, M. T. & Kirchman, D. L. (2000). Natural assemblages of marine proteobacteria and members of the Cytophaga-Flavobacter cluster consuming low-and high-molecular-weight dissolved organic matter. *Applied and Environmental Microbiology*, *66*(4), 1692–1697.

Croft, M. T., Lawrence, A. D., Raux-Deery, E., Warren, M. J. & Smith, A. G. (2005). Algae acquire vitamin B12 through a symbiotic relationship with bacteria. *Nature*, *438*(7064), 90–93. https://doi.org/10.1038/nature04056

De Cáceres, M. & Legendre, P. (2009). Associations between species and groups of sites: Indices and statistical inference. *Ecology*, *90*(12), 3566–3574. https://doi.org/10.1890/08-1823.1

Eiler, A., Gonzalez-Rey, C., Allen, S. & Bertilsson, S. (2007). Growth response of Vibrio cholerae and other Vibrio spp. to cyanobacterial dissolved organic matter and temperature in brackish water. *FEMS Microbiology Ecology*, *60*(3), 411–418. https://doi.org/10.1111/j.1574-6941.2007.00303.x

Dupont, C. L., Rusch, D. B., Yooseph, S., Lombardo, M.-J., Alexander Richter, R., Valas, R., Novotny, M., Yee-Greenbaum, J., Selengut, J. D., Haft, D. H., Halpern, A. L., Lasken, R. S., Nealson, K., Friedman, R. & Craig Venter, J. (2012). Genomic insights to SAR86, an abundant and uncultivated marine bacterial lineage. *The ISME Journal*, *6*(6), 1186–1199. https://doi.org/10.1038/ismej.2011.189

Falkowski, P. G. (1994). *The role of phytoplankton photosynthesis in global biogeochemical cycles*. 235–258.

Fernández-Gomez, B., Richter, M., Schüler, M., Pinhassi, J., Acinas, S. G., González, J. M. & Pedros-Alio, C. (2013). Ecology of marine Bacteroidetes: a comparative genomics approach. *The ISME Journal*, *7*(5), 1026–1037.

Field, C. B., Behrenfeld, M. J., Randerson, J. T. & Falkowski, P. (1998). Primary Production of the Biosphere: Integrating Terrestrial and Oceanic Components. *Science*, *281*(5374), 237 LP – 240. https://doi.org/10.1126/science.281.5374.237

Fisher, C. L., Lane, P. D., Russell, M., Maddalena, R. & Lane, T. W. (2020). Low Molecular Weight Volatile Organic Compounds Indicate Grazing by the Marine Rotifer Brachionus plicatilis on the Microalgae Microchloropsis salina. *Metabolites*, *10*(9), 361.

Francis, T. Ben, Bartosik, D., Sura, T., Sichert, A., Hehemann, J.-H., Markert, S., Schweder, T., Fuchs, B. M., Teeling, H. & Amann, R. I. (2021). Changing expression patterns of TonB-dependent transporters suggest shifts in polysaccharide consumption over the course of a spring phytoplankton bloom. *The ISME Journal*, 1–15.

Fu, H., Uchimiya, M., Gore, J. & Moran, M. A. (2020). Ecological drivers of bacterial community assembly in synthetic phycospheres. Proceedings of the National Academy of Sciences of the United States of America, 117(7), 3656–3662. https://doi.org/10.1073/pnas.1917265117

Gilbert, J. A., Steele, J. A., Caporaso, J. G., Steinbrück, L., Reeder, J., Temperton, B., Huse, S., McHardy, A. C., Knight, R., Joint, I., Somerfield, P., Fuhrman, J. A. & Field, D. (2012). Defining seasonal marine microbial community dynamics. *The ISME Journal*, *6*(2), 298–308. https://doi.org/10.1038/ismej.2011.107

Giovannoni, S. J., Hayakawa, D. H., Tripp, H. J., Stingl, U., Givan, S. A., Cho, J. C., Oh, H. M., Kitner, J. B., Vergin, K. L. & Rappé, M. S. (2008). The small genome of an abundant coastal ocean methylotroph. Environmental Microbiology, 10(7), 1771–1782. https://doi.org/10.1111/j.1462-2920.2008.01598.x

Glasl, B., Herndl, G. J. & Frade, P. R. (2016). The microbiome of coral surface mucus has a key role in mediating holobiont health and survival upon disturbance. *ISME Journal*, *10*(9), 2280–2292. https://doi.org/10.1038/ismej.2016.9

Gohin, F., Van der Zande, D., Tilstone, G., Eleveld, M. A., Lefebvre, A., Andrieux-Loyer, F., Blauw, A. N., Bryère, P., Devreker, D., Garnesson, P., Hernández Fariñas, T., Lamaury, Y., Lampert, L., Lavigne, H., Menet-Nedelec, F., Pardo, S. & Saulquin, B. (2019). Twenty years of satellite and in situ observations of surface chlorophyll-a from the northern Bay of Biscay to the eastern English Channel. Is the water quality improving? *Remote Sensing of Environment*, *233*(July), 111343. https://doi.org/10.1016/j.rse.2019.111343

Gonzalez, J. M., Simó, R., Massana, R., Covert, J. S., Casamayor, E. O., Pedrós-Alió, C. & Moran, M. A. (2000). Bacterial community structure associated with a dimethylsulfoniopropionate-producing North Atlantic algal bloom. *Appl. Environ. Microbiol.*, *66*(10), 4237–4246. https://doi.org/10.1128/AEM.66.10.4237-4246.2000

Green, D. H., Echavarri-Bravo, V., Brennan, D. & Hart, M. C. (2015). Bacterial diversity associated with the coccolithophorid algae Emiliania huxleyi and Coccolithus pelagicus f. braarudii. *BioMed Research International*, *2015*. https://doi.org/10.1155/2015/194540

Hahnke, R. L., Bennke, C. M., Fuchs, B. M., Mann, A. J., Rhiel, E., Teeling, H., Amann, R. & Harder, J. (2015). *Dilution cultivation of marine heterotrophic bacteria abundant after a spring phytoplankton bloom in the North Sea*. *17*, 3515–3526. https://doi.org/10.1111/1462-2920.12479

Holligan, P. M., Viollier, M., Harbour, D. S., Camus, P. & Champagne-Philippe, M. (1983). Satellite and ship studies of coccolithophore production along a continental shelf edge. *Nature*, *304*(5924), 339–342.

Holmström, C. & Kjelleberg, S. (1999). Marine Pseudoalteromonas species are associated with higher organisms and produce biologically active extracellular agents. *FEMS Microbiology Ecology*, *30*(4), 285–293.

Hunter, J. E., Frada, M. J., Fredricks, H. F., Vardi, A. & Van Mooy, B. A. S. (2015). Targeted and untargeted lipidomics of Emiliania huxleyi viral infection and life cycle phases highlights molecular biomarkers of infection, susceptibility, and ploidy. *Frontiers in Marine Science*, *2*, 81.

Jackrel, S. L., Yang, J. W., Schmidt, K. C. & Denef, V. J. (2020). Host specificity of microbiome assembly and its fitness effects in phytoplankton. *The ISME Journal*. https://doi.org/10.1038/s41396-020-00812-x

Kappelmann, L., Krüger, K., Hehemann, J. H., Harder, J., Markert, S., Unfried, F., Becher, D., Shapiro, N., Schweder, T., Amann, R. I. & Teeling, H. (2019). Polysaccharide utilization loci of North Sea Flavobacteriia as basis for using SusC/D-protein expression for predicting major phytoplankton glycans. *ISME Journal*, *13*(1), 76–91. https://doi.org/10.1038/s41396-018-0242-6

Keuter, S., Young, J. R. & Frada, M. J. (2019). Life cycle association of the coccolithophore Syracosphaera gaarderae comb. nov. (ex Alveosphaera bimurata): Taxonomy, ecology and evolutionary implications. *Marine Micropaleontology*, *148*(March), 58–64. https://doi.org/10.1016/j.marmicro.2019.03.007

Kim, J.-G., Gwak, J.-H., Jung, M.-Y., An, S.-U., Hyun, J.-H., Kang, S. & Rhee, S.-K. (2019). Distinct temporal dynamics of planktonic archaeal and bacterial assemblages in the bays of the Yellow Sea. *PLOS ONE*, *14*(8), e0221408. https://doi.org/10.1371/journal.pone.0221408

Kimbrel, J. A., Samo, T. J., Ward, C., Nilson, D., Thelen, M. P., Siccardi, A., Zimba, P., Lane, T. W. & Mayali, X. (2019). Host selection and stochastic effects influence bacterial community assembly on the microalgal phycosphere. *Algal Research*, *40*, 101489. https://doi.org/10.1016/J.ALGAL.2019.101489

Kindt, R. & Coe, R. (2005). Tree diversity analysis. A manual and software for common statistical methods for ecological and biodiversity studies. *World Agroforestry Centre (ICRAF), ISBN 92-9059-179-X*.

Kirchman, D. L. (2002). The ecology of Cytophaga–Flavobacteria in aquatic environments. *FEMS Microbiology Ecology*, *39*(2), 91–100.

Krüger, K., Chafee, M., Ben Francis, T., Glavina del Rio, T., Becher, D., Schweder, T., Amann, R. I. & Teeling, H. (2019). In marine Bacteroidetes the bulk of glycan degradation during algae blooms is mediated by few clades using a restricted set of genes. *ISME Journal*, *13*(11), 2800–2816. https://doi.org/10.1038/s41396-019-0476-y

Laber, C. P., Hunter, J. E., Carvalho, F., Collins, J. R., Hunter, E. J., Schieler, B. M., Boss, E., More, K., Frada, M., Thamatrakoln, K., Brown, C. M., Haramaty, L., Ossolinski, J., Fredricks, H., Nissimov, J. I., Vandzura, R., Sheyn, U., Lehahn, Y., Chant, R. J., … Bidle, K. D. (2018). Coccolithovirus facilitation of carbon export in the North Atlantic. *Nature Microbiology*, 1–11. https://doi.org/10.1038/s41564-018-0128-4

Landa, M., Blain, S., Christaki, U., Monchy, S. & Obernosterer, I. (2016). Shifts in bacterial community composition associated with increased carbon cycling in a mosaic of phytoplankton blooms. *ISME Journal*, *10*(1), 39–50. https://doi.org/10.1038/ismej.2015.105

Lawson, C. A., Raina, J. B., Kahlke, T., Seymour, J. R. & Suggett, D. J. (2018). Defining the core microbiome of the symbiotic dinoflagellate, Symbiodinium. *Environmental Microbiology Reports*, *10*(1), 7–11. https://doi.org/10.1111/1758-2229.12599

Legendre, P. & Gallagher, E. D. (2001). Ecologically meaningful transformations for ordination of species data. *Oecologia*, *129*(2), 271–280.

Lehahn, Y., Koren, I., Schatz, D., Frada, M., Sheyn, U., Boss, E., Efrati, S., Rudich, Y., Trainic, M., Sharoni, S., Laber, C., Ditullio, G. R., Coolen, M. J. L., Martins, A. M., Van Mooy, B. A. S., Bidle, K. D. & Vardi, A. (2014). Decoupling physical from biological processes to assess the impact of viruses on a mesoscale algal bloom. *Current Biology*, *24*(17), 2041–2046. https://doi.org/10.1016/j.cub.2014.07.046

Li, D. X., Zhang, H., Chen, X. H., Xie, Z. X., Zhang, Y., Zhang, S. F., Lin, L., Chen, F. & Wang, D. Z. (2018). Metaproteomics reveals major microbial players and their metabolic activities during the blooming period of a marine dinoflagellate Prorocentrum donghaiense. *Environmental Microbiology*, *20*(2), 632–644. https://doi.org/10.1111/1462-2920.13986

Liu, Y., Blain, S., Crispi, O., Rembauville, M. & Obernosterer, I. (2020). Seasonal dynamics of prokaryotes and their associations with diatoms in the Southern Ocean as revealed by an autonomous sampler. *Environmental Microbiology*, *22*(9), 3968–3984.

Longford, S. R., Campbell, A. H., Nielsen, S., Case, R. J., Kjelleberg, S. & Steinberg, P. D. (2019). Interactions within the microbiome alter microbial interactions with host chemical

defences and affect disease in a marine holobiont. *Scientific Reports*, *9*(1), 1–13. https://doi.org/10.1038/s41598-018-37062-z

Lovejoy, C., Bowman, J. P. & Hallegraeff, G. M. (1998). Algicidal effects of a novel marine Pseudoalteromonas isolate (class Proteobacteria, gamma subdivision) on harmful algal bloom species of the genera Chattonella, Gymnodinium, and Heterosigma. *Applied and Environmental Microbiology*, *64*(8), 2806–2813. https://doi.org/10.1128/aem.64.8.2806-2813.1998

Lucas, J., Koester, I., Wichels, A., Niggemann, J., Dittmar, T., Callies, U., Wiltshire, K. H. & Gerdts, G. (2016). Short-term dynamics of North Sea bacterioplankton-dissolved organic matter coherence on molecular level. *Frontiers in Microbiology*, *7*, 321.

Malin, G., Turner, S., Liss, P., Holligan, P. & Harbour, D. (1993). Dimethylsulphide and dimethylsulphoniopropionate in the Northeast Atlantic during the summer coccolithophore bloom. *Deep-Sea Research Part I*, *40*, 1487–1508. https://doi.org/doi:10.1016/0967-0637 (93)90125-M

Malin, Gill & Steinke, M. (2004). Dimethyl sulfide production: what is the contribution of the coccolithophores? *Coccolithophores*, 127–164. https://doi.org/10.1007/978-3-662-06278-4_6

Marie, D., Brussaard, C. P. D., Partensky, F. & Vaulot, D. (1999). Flow cytometric analysis of phytoplankton, bacteria and viruses. *Current Protocols in Cytometry*, *11.11*, 1–15.

Martin, M. (2011). Cutadapt removes adapter sequences from high-throughput sequencing reads. *EMBnet.Journal; Vol 17, No 1: Next Generation Sequencing Data AnalysisDO - 10.14806/Ej.17.1.200* . http://journal.embnet.org/index.php/embnetjournal/article/view/200

Mena, C., Reglero, P., Balbín, R., Martín, M., Santiago, R. & Sintes, E. (2020). Seasonal Niche Partitioning of Surface Temperate Open Ocean Prokaryotic Communities . In *Frontiers in Microbiology* (Vol. 11). https://www.frontiersin.org/articles/10.3389/fmicb.2020.01749

Meyer, N., Bigalke, A., Kaulfuß, A. & Pohnert, G. (2017). Strategies and ecological roles of algicidal bacteria. *FEMS Microbiology Reviews*, *41*(6), 880–899. https://doi.org/10.1093/femsre/fux029

Miller, T. R. & Belas, R. (2004). Dimethylsulfoniopropionate Metabolism by *Pfiesteria* -Associated *Roseobacter spp .†*. *70*(6), 3383–3391. https://doi.org/10.1128/AEM.70.6.3383

Mönnich, J., Tebben, J., Bergemann, J., Case, R., Wohlrab, S. & Harder, T. (2020). Niche-based assembly of bacterial consortia on the diatom Thalassiosira rotula is stable and reproducible. *The ISME Journal*, *14*, 1614–1625. https://doi.org/10.1038/s41396-020-0631-5

Murali, A., Bhargava, A. & Wright, E. S. (2018). IDTAXA: a novel approach for accurate taxonomic classification of microbiome sequences. *Microbiome*, *6*(1), 140. https://doi.org/10.1186/s40168-018-0521-5

Neufeld, J. D., Boden, R., Moussard, H., Schäfer, H. & Murrell, J. C. (2008). Substrate-specific clades of active marine methylotrophs associated with a phytoplankton bloom in a temperate coastal environment. *Applied and Environmental Microbiology*, *74*(23), 7321–7328. https://doi.org/10.1128/AEM.01266-08

Neukermans, G. & Fournier, G. (2018). Optical modeling of spectral backscattering and remote sensing reflectance from Emiliania huxleyi Blooms. *Frontiers in Marine Science*, *5*(MAY), 1–20. https://doi.org/10.3389/fmars.2018.00146

Oksanen, J., Blanchet, F. G., Kindt, R., Legendre, P., Minchin, P. R., O'Hara, R. B., Simpson, G. L., Solymos, P., Stevens, M. H. H. & Wagner, H. (2015). OK-Package 'vegan.' *Community Ecology Package, Version*, 285 pp.

Orata, F. D., Rosana, A. R. R., Xu, Y., Simkus, D. N., Bramucci, A. R., Boucher, Y. & Case, R. J. (2016). *Polymicrobial Culture of Naked (N-Type) Emiliania huxleyi*. *4*(4), 9–10. https://doi.org/10.1128/genomeA.00674-16.Copyright

Orellana, L. H., Ben Francis, T., Krüger, K., Teeling, H., Müller, M.-C., Fuchs, B. M., Konstantinidis, K. T. & Amann, R. I. (2019). Niche differentiation among annually recurrent coastal Marine Group II Euryarchaeota. *The ISME Journal*, *13*(12), 3024–3036. https://doi.org/10.1038/s41396-019-0491-z

Parada, A. E., Needham, D. M. & Fuhrman, J. A. (2016). Every base matters: Assessing small subunit rRNA primers for marine microbiomes with mock communities, time series and global field samples. *Environmental Microbiology*, *18*(5), 1403–1414. https://doi.org/10.1111/1462-2920.13023

Paradis, E. & Schliep, K. (2019). ape 5.0: an environment for modern phylogenetics and evolutionary analyses in R. *Bioinformatics*, *35*(3), 526–528.

Perrot, L., Gohin, F., Ruiz-Pino, D., Lampert, L., Huret, M., Dessier, A., Malestroit, P., Dupuy, C. & Bourriau, P. (2018). Coccolith-derived turbidity and hydrological conditions in May in the Bay of Biscay. *Progress in Oceanography*, *166*, 41–53.

Pomeroy, L., leB. Williams, P., Azam, F. & Hobbie, J. (2007). The Microbial Loop. *Oceanography*, *20*(2), 28–33. https://doi.org/10.5670/oceanog.2007.45

Poulton, A. J., Stinchcombe, M. C., Achterberg, E. P., Bakker, D. C. E., Dumousseaud, C., Lawson, H. E., Lee, G. A., Richier, S., Suggett, D. J. & Young, J. R. (2014). Coccolithophores on the north-west European shelf: calcification rates and environmental controls. *Biogeosciences*, *11*(14), 3919–3940.

Quast, C., Pruesse, E., Yilmaz, P., Gerken, J., Schweer, T., Yarza, P., Peplies, J. & Glöckner, F. O. (2013). The SILVA ribosomal RNA gene database project: improved data processing and web-based tools. *Nucleic Acids Research*, *41*(D1), D590–D596.

R Core Team. (2017). *R: A language and environment for statistical computing. R Foundation for Statistical Computing, Vienna, Austria. URL https://www.R-project.org/*.

Reese, K. L., Fisher, C. L., Lane, P. D., Jaryenneh, J. D., Moorman, M. W., Jones, A. D., Frank, M. & Lane, T. W. (2019). Chemical profiling of volatile organic compounds in the headspace of algal cultures as early biomarkers of algal pond crashes. *Scientific Reports*, *9*(1), 1–10.

Reintjes, G., Arnosti, C., Fuchs, B. & Amann, R. (2019). Selfish, sharing and scavenging bacteria in the Atlantic Ocean: a biogeographical study of bacterial substrate utilisation. *The ISME Journal*, *13*(5), 1119–1132. https://doi.org/10.1038/s41396-018-0326-3

Rognes, T., Flouri, T., Nichols, B., Quince, C. & Mahé, F. (2016). VSEARCH: a versatile open source tool for metagenomics. *PeerJ*, *4*, e2584–e2584. https://doi.org/10.7717/peerj.2584

Romac, S. (2022a). Cryogrinding protocol : mecanic lysis of planktonic filter for RNA/DNA extraction. *Protocols.Io*. https://doi.org/https://dx.doi.org/10.17504/protocols.io.beqpjdvn

Romac, S. (2022b). Prokaryotes 16S-V4V5 rRNA Metabarcoding PCR protocol for NGS Illumina sequencing. *Protocols.Io*. https://doi.org/https://dx.doi.org/10.17504/protocols.io.bzwwp7fe

Romac, S. (2022c). RNA/DNA extraction from plankton natural samples using NucleoSpin RNA + RNA/DNA Buffer kits (Macherey Nagel). *Protocols.Io*. https://doi.org/https://dx.doi.org/10.17504/protocols.io.b2j7qcrn

Romac, S. (2022d). Total DNA extraction from microalgae strain samples using NucleoSpin Plant modified kit (Macherey Nagel). *Protocols.Io*. https://doi.org/https://dx.doi.org/10.17504/protocols.io.b2ctqawn

Rosana, A. R. R., Orata, F. D., Xu, Y., Simkus, D. N., Bramucci, A. R., Boucher, Y. & Case, R. J. (2016). Draft genome sequences of seven bacterial strains isolated from a

polymicrobial culture of coccolith-bearing (C-type) Emiliania huxleyi M217. *Genome Announcements*, *4*(4).
Rost, B., Riebesell, U., Röst, B. & Riebesell, U. (2004). Coccolithophores and the biological pump: Responses to environmental changes. *Coccolithophores: From Molecular Processes to Global Impact*, 99–125. https://doi.org/10.1007/978-3-662-06278-4_5
RStudio Team. (2016). RStudio: Integrated Development for R. *RStudio, Inc., Boston, MA*. http://www.rstudio.com/.
Saary, P., Forslund, K., Bork, P. & Hildebrand, F. (2017). *RTK: efficient rarefaction analysis of large datasets.* (R package version 0.2.6.1). https://doi.org/doi: 10.1093/bioinformatics/btx206
Seyedsayamdost, M. R., Wang, R., Kolter, R. & Clardy, J. (2014). Hybrid biosynthesis of roseobacticides from algal and bacterial precursor molecules. *Journal of the American Chemical Society*, *136*(43), 15150–15153. https://doi.org/10.1021/ja508782y
Seymour, J. R., Amin, S. A., Raina, J. B. & Stocker, R. (2017). Zooming in on the phycosphere: The ecological interface for phytoplankton-bacteria relationships. *Nature Microbiology*, *2*(May). https://doi.org/10.1038/nmicrobiol.2017.65
Shibl, A. A., Isaac, A., Ochsenkühn, M. A., Cárdenas, A., Fei, C., Behringer, G., Arnoux, M., Drou, N., Santos, M. P., Gunsalus, K. C., Voolstra, C. R. & Amin, S. A. (2020). Diatom modulation of select bacteria through use of two unique secondary metabolites. *Proceedings of the National Academy of Sciences of the United States of America*, *117*(44), 27445–27455. https://doi.org/10.1073/pnas.2012088117
Smriga, S., Fernandez, V. I., Mitchell, J. G. & Stocker, R. (2016). Chemotaxis toward phytoplankton drives organic matter partitioning among marine bacteria. *Proceedings of the National Academy of Sciences of the United States of America*, *113*(6), 1576–1581. https://doi.org/10.1073/pnas.1512307113
Sonnenschein, E. C., Syit, D. A., Grossart, H. P. & Ullrich, M. S. (2012). Chemotaxis of Marinobacter adhaerens and its impact on attachmentto the diatom Thalassiosira weissflogii. *Applied and Environmental Microbiology*, *78*(19), 6900–6907. https://doi.org/10.1128/AEM.01790-12
Sörenson, E., Bertos-Fortis, M., Farnelid, H., Kremp, A., Krüger, K., Lindehoff, E. & Legrand, C. (2019). Consistency in microbiomes in cultures of Alexandrium species isolated from brackish and marine waters. *Environmental Microbiology Reports*, *11*(3), 425–433. https://doi.org/10.1111/1758-2229.12736
Spring, S. & Riedel, T. (2013). Mixotrophic growth of bacteriochlorophyll a-containing members of the OM60/NOR5 clade of marine gammaproteobacteria is carbon-starvation independent and correlates with the type of carbon source and oxygen availability. *BMC Microbiology*, *13*(1), 1. https://doi.org/10.1186/1471-2180-13-117
Stock, W., Willems, A., Mangelinckx, S., Vyverman, W. & Sabbe, K. (2022). Selection constrains lottery assembly in the microbiomes of closely related diatom species. *ISME Communications*, *2*(1), 11. https://doi.org/10.1038/s43705-022-00091-x
Sunagawa, S., Acinas, S. G., Bork, P., Bowler, C., Acinas, S. G., Babin, M., Bork, P., Boss, E., Bowler, C., Cochrane, G., de Vargas, C., Follows, M., Gorsky, G., Grimsley, N., Guidi, L., Hingamp, P., Iudicone, D., Jaillon, O., Kandels, S., … Coordinators, T. O. (2020). Tara Oceans: towards global ocean ecosystems biology. *Nature Reviews Microbiology*, *18*(8), 428–445. https://doi.org/10.1038/s41579-020-0364-5
Teeling, H., Fuchs, B. M., Becher, D., Klockow, C., Gardebrecht, A., Bennke, C. M., Kassabgy, M., Huang, S., Mann, A. J., Waldmann, J., Weber, M., Klindworth, A., Otto, A., Lange, J., Bernhardt, J., Reinsch, C., Hecker, M., Peplies, J., Bockelmann, F. D., … Amann, R. (2012). Substrate-controlled succession of marine bacterioplankton populations induced by a phytoplankton bloom. *Science*, *336*(6081), 608–611.

https://doi.org/10.1126/science.1218344
Teeling, H., Fuchs, B. M., Bennke, C. M., Krüger, K., Chafee, M., Kappelmann, L., Reintjes, G., Waldmann, J., Quast, C., Glöckner, F. O., Lucas, J., Wichels, A., Gerdts, G., Wiltshire, K. H. & Amann, R. I. (2016). Recurring patterns in bacterioplankton dynamics during coastal spring algae blooms. *ELife*, *5*, 1–31. https://doi.org/10.7554/eLife.11888
Thompson, H. F., Summers, S., Yuecel, R. & Gutierrez, T. (2020). Hydrocarbon-degrading bacteria found tightly associated with the 50–70 µm cell-size population of eukaryotic phytoplankton in surface waters of a northeast atlantic region. *Microorganisms*, *8*(12), 1–16. https://doi.org/10.3390/microorganisms8121955
Tréguer, P. & Le Corre, P. (1975). Manuel d'analyse des sels nutritifs dans l'eau de mer (utilisation de l'autoanalyseur Technicon R). *Rapport de l'Universite de Bretagne Occidentale*.
Treusch, A. H., Vergin, K. L., Finlay, L. A., Donatz, M. G., Burton, R. M., Carlson, C. A. & Giovannoni, S. J. (2009). Seasonality and vertical structure of microbial communities in an ocean gyre. *The ISME Journal*, *3*(10), 1148–1163. https://doi.org/10.1038/ismej.2009.60
Tripp, H. J., Kitner, J. B., Schwalbach, M. S., Dacey, J. W. H., Wilhelm, L. J. & Giovannoni, S. J. (2008). SAR11 marine bacteria require exogenous reduced sulphur for growth. *Nature*, *452*(7188), 741–744. https://doi.org/10.1038/nature06776
Tyrrell, T. & Merico, A. (2004). *Emiliania huxleyi*: bloom observations and the conditions that induce them. In *Coccolithophores* (pp. 75–97). https://doi.org/10.1007/978-3-662-06278-4_4
Vardi, A., Haramaty, L., Van Mooy, B. A. S., Fredricks, H. F., Kimmance, S. A., Larsen, A. & Bidle, K. D. (2012). Host-virus dynamics and subcellular controls of cell fate in a natural coccolithophore population. *Proceedings of the National Academy of Sciences of the United States of America*, *109*(47), 19327–19332. https://doi.org/10.1073/pnas.1208895109
Vardi, A., Van Mooy, B. A. S., Fredricks, H. F., Popendorf, K. J., Ossolinski, J. E., Haramaty, L. & Bidle, K. D. (2009). Viral glycosphingolipids induce lytic infection and cell death in marine phytoplankton. *Science*, *326*(5954), 861–865.
Vincent, F., Sheyn, U., Porat, Z., Schatz, D. & Vardi, A. (2021). Visualizing active viral infection reveals diverse cell fates in synchronized algal bloom demise. *Proceedings of the National Academy of Sciences*, *118*(11), e2021586118. https://doi.org/10.1073/pnas.2021586118
Wemheuer, B., Wemheuer, F., Hollensteiner, J., Meyer, F.-D., Voget, S. & Daniel, R. (2015). The green impact: bacterioplankton response toward a phytoplankton spring bloom in the southern North Sea assessed by comparative metagenomic and metatranscriptomic approaches. In *Frontiers in Microbiology* (Vol. 6). https://www.frontiersin.org/article/10.3389/fmicb.2015.00805
Wickham, H. (2016). ggplot2: Elegant Graphics for Data Analysis. *Springer-Verlag New York*, *ISBN 978-3*. https://ggplot2.tidyverse.org
Yang, S.-J., Kang, I. & Cho, J.-C. (2016). Expansion of cultured bacterial diversity by large-scale dilution-to-extinction culturing from a single seawater sample. *Microbial Ecology*, *71*(1), 29–43.
Zhou, J., Chen, G. F., Ying, K. Z., Jin, H., Song, J. T. & Cai, Z. H. (2019). Phycosphere microbial succession patterns and assembly mechanisms in a marine dinoflagellate bloom. *Applied and Environmental Microbiology*, *85*(15), 1–17. https://doi.org/10.1128/AEM.00349-19
Ziv, C., Malitsky, S., Othman, A., Ben-Dor, S., Wei, Y., Zheng, S., Aharoni, A., Hornemann, T. & Vardi, A. (2016). Viral serine palmitoyltransferase induces metabolic switch in

sphingolipid biosynthesis and is required for infection of a marine alga. *Proceedings of the National Academy of Sciences*, *113*(13), E1907–E1916.

Zubkov, M. V., Fuchs, B. M., Archer, S. D., Kiene, R. P., Amann, R. & Burkill, P. H. (2001). Linking the composition of bacterioplankton to rapid turnover of dissolved dimethylsulphoniopropionate in an algal bloom in the North Sea. *Environmental Microbiology*, *3*(5), 304–311. https://doi.org/10.1046/j.1462-2920.2001.00196.x

Figures and Captions

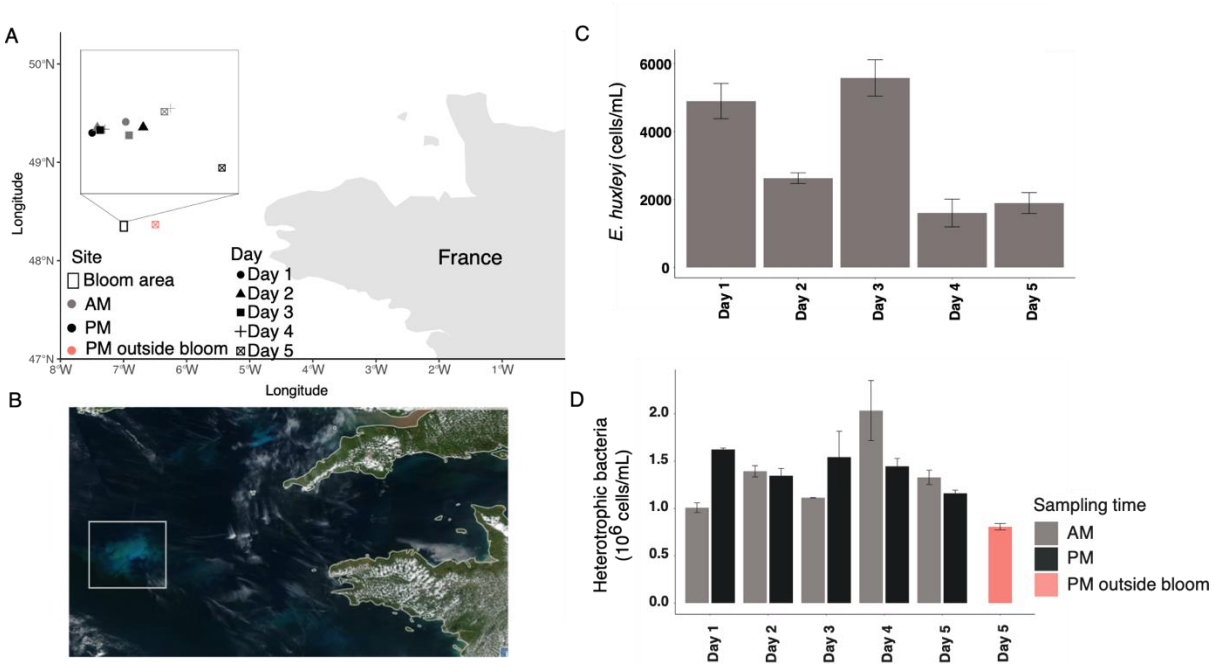

Fig. 1. Sampling area and characteristics of the *E. huxleyi* bloom in the Celtic Sea. **A)** Map showing the bloom area and spatio-temporal sampling strategy (AM and PM denote morning and afternoon samplings). **B)** True-color satellite image of the bloom area on May 21, 2019 (source: https://www.star.nesdis.noaa.gov/sod/mecb/color/ocview/ocview.html. **C)** *E. huxleyi* cell concentrations at morning bloom sites during the survey, measured from duplicate filters using scanning electron microscopy. **D)** Heterotrophic bacterial cell concentrations at morning and afternoon sites during the survey, measured from duplicate samples by flow cytometry.

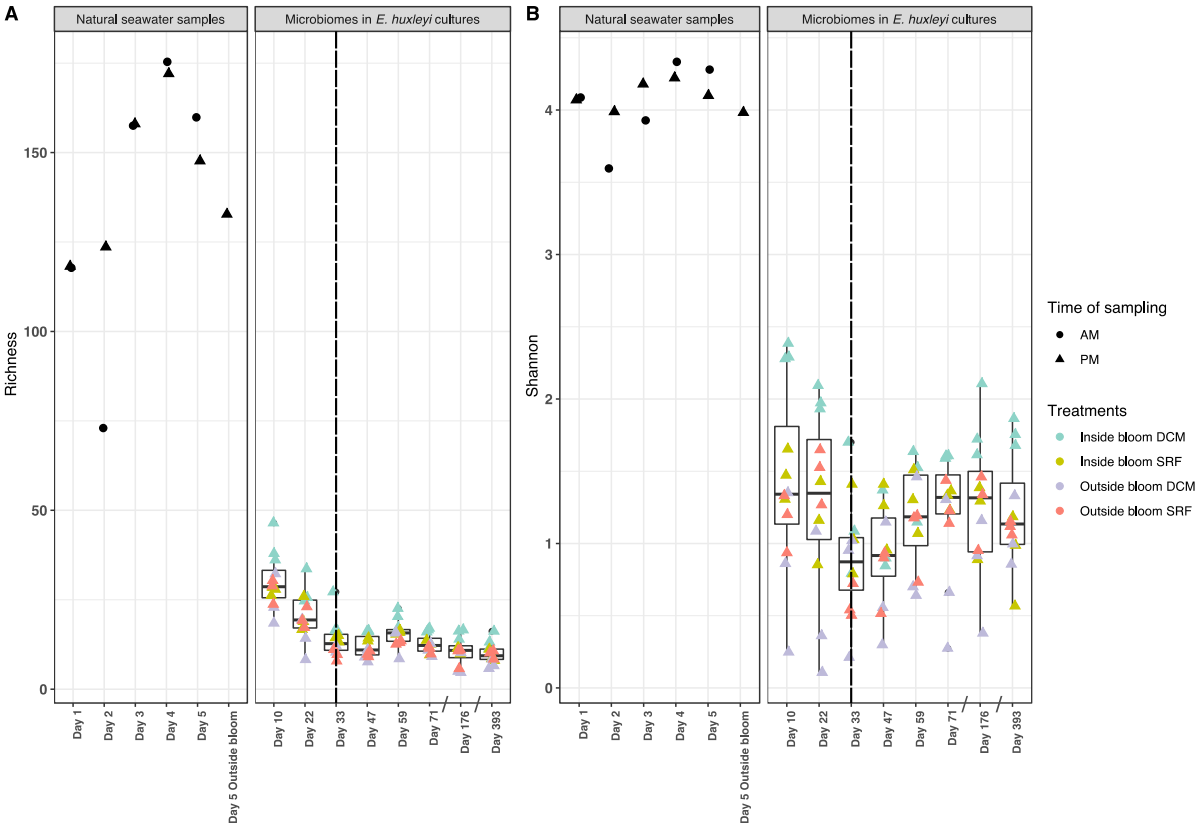

Fig. 2. Composite representation of the dynamics of the prokaryotic richness **(A)** and Shannon **(B)** indexes in natural samples (0.2 – 3 µm DCM samples only) and culture experiments. ASV tables were rarefied to 2,479 (minimum number of reads of the environmental samples. The boxes represent the interquartile range. The thin horizontal lines represent the 25th and 75th percentiles and while the thick horizontal line represents the median. The vertical lines indicate the minimum and maximum values (using 1.5 coefficients above and below the percentiles). The dots represent the values measured for each culture. Dots further than the vertical lines represent potential outliers. X-axis in the in the experiment plot are not proportional to the time length between samplings. The black dotted line represents the time where the cultivation conditions changed.

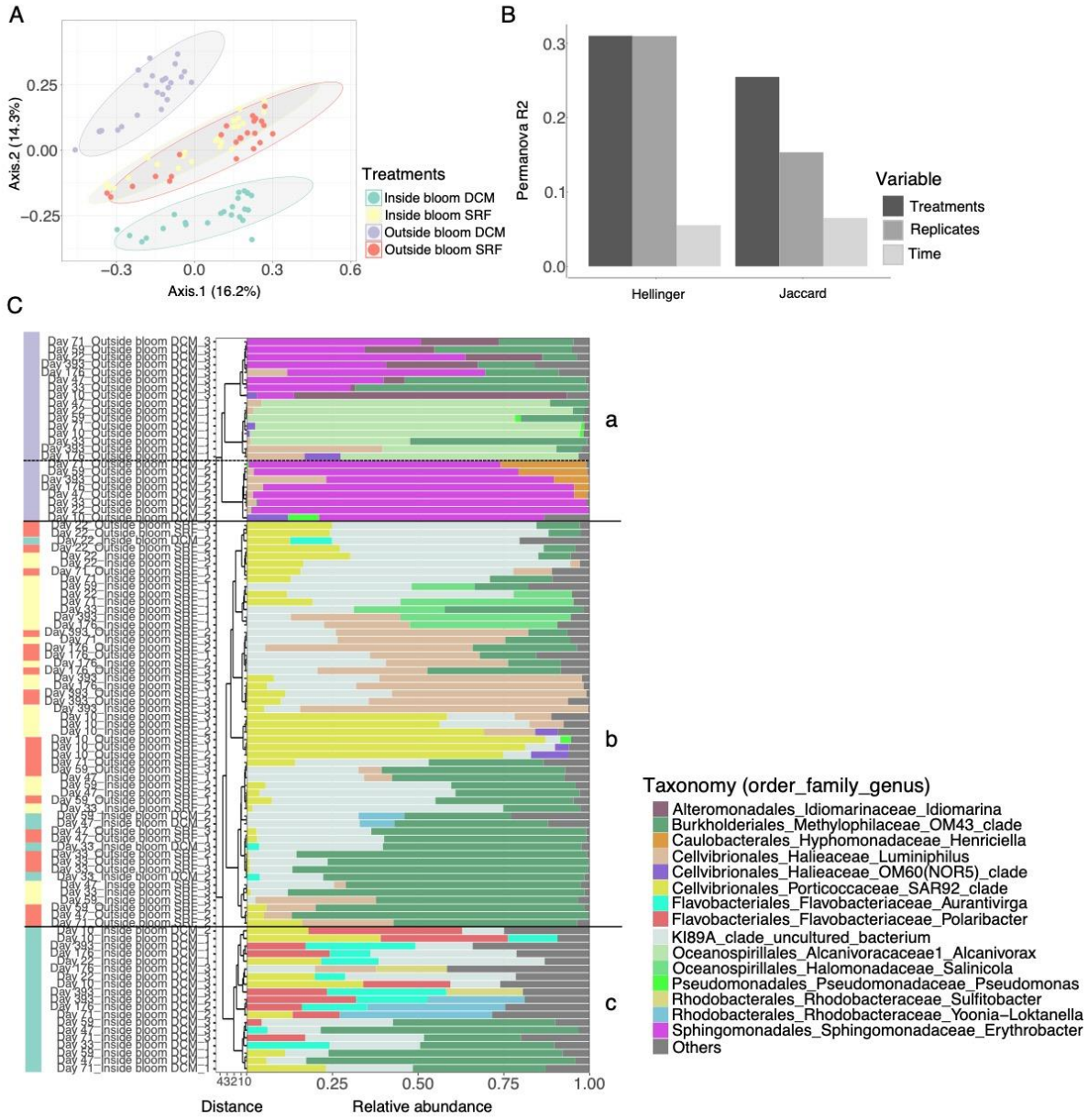

Fig. 3. Beta diversity patterns of *E. huxleyi* microbiomes across treatments and time. (A) Principal coordinates analysis (PcoA) using Jaccard dissimilarity matrix of the presence-absence transformed rarefied table. Colors correspond to each treatment that received prokaryotic communities from different water samples: green - Inside bloom DCM; yellow - Inside bloom surface (SRF); purple - Outside bloom DCM; red - Outside bloom SRF. Ellipses represent 95% confidence. (B) Permutational multivariate analysis of variance (PERMANOVA) and nested PERMANOVA r^2 of significant variables ($p < 0.01$) using both metrics (see Supplementary Tables 3 and 4 for detailed results). (C) Hierarchical clustering produced with the Hellinger distance matrix using "ward.D2" method. Codes of each microbiome are experiment sampling day_treatment_replicate. On the left, colors used for each treatment are the same than in Fig. 3A. Bar plots indicate the taxonomy of the 3 most abundant genera. The other genera were merged as "others".

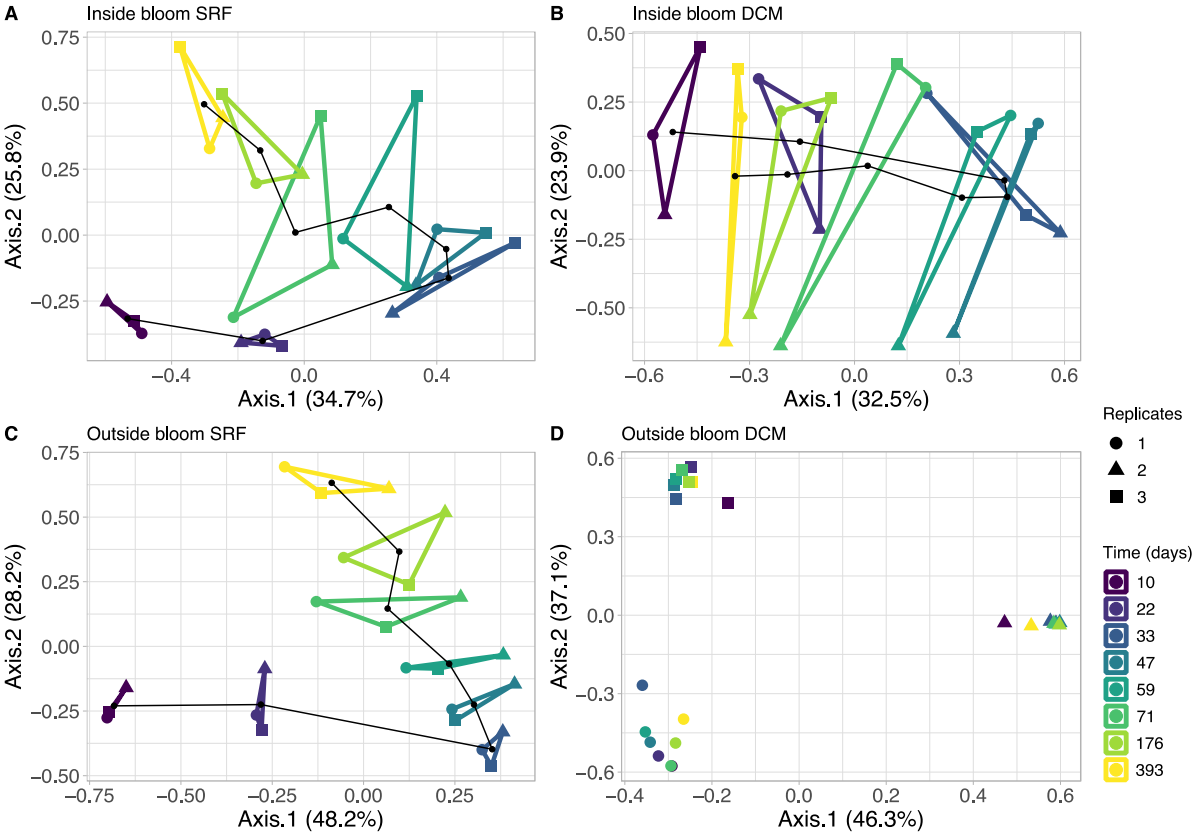

Fig. 4. Principal component analysis (PCA) showing the cyclic patterns of the microbiome beta diversity. Community distances (Euclidean distances of Hellinger-transformed data) are shown for microbiomes from inside bloom surface (SRF) (A), inside bloom DCM (B), outside bloom SRF (C), and outside bloom DCM (D). The polygons link replicates (shape coded) at each DNA sampling (color coded). The black line links the barycenters of the replicates.